



Published in final edited form as:

Biol Psychiatry. 2016 August 1; 80(3): 207–215. doi:10.1016/j.biopsych.2015.12.022.

Cocaine self-administration and extinction leads to reduced GFAP expression and morphometric features of astrocytes in the nucleus accumbens core

Michael D. Scofield¹, Hao Li^{1,*}, Benjamin Siemsen^{1,*}, Kati L. Healey², Phuong K. Tran¹, Nicholas Woronoff², Heather A. Boger¹, Peter W. Kalivas¹, and Kathryn J. Reissner^{2,3}

¹Department of Neurosciences, Medical University of South Carolina, Charleston, SC

²Department of Psychology and Neuroscience, UNC Chapel Hill, Chapel Hill, NC

³Department of Psychology and Neuroscience, UNC Chapel Hill, Chapel Hill, NC

Abstract

Background—As a more detailed picture of nervous system function emerges, diversity of astrocyte function becomes more widely appreciated. While it has been shown that cocaine experience impairs astroglial glutamate uptake and release in the nucleus accumbens (NAc), few studies have explored effects of self-administration on the structure and physiology of astrocytes. We investigated the effects of extinction from daily cocaine self-administration on astrocyte characteristics including GFAP expression, surface area, volume, and colocalization with a synaptic marker.

Methods—Cocaine or saline self-administration and extinction were paired with GFAP Westerns, immunohistochemistry, and fluorescent imaging of NAc core astrocytes (30 saline-administering and 36 cocaine-administering male Sprague Dawley rats were employed). Imaging was performed using a membrane-tagged Lck-GFP driven by the GFAP promoter, coupled with synapsin I immunohistochemistry.

Results—GFAP expression was significantly reduced in the NAc core following cocaine self-administration and extinction. Similarly, we observed an overall smaller surface area and volume of astrocytes, as well as reduced colocalization with synapsin I, in cocaine-administering animals. Cocaine-mediated reductions in synaptic contact were reversed by the β -lactam antibiotic ceftriaxone.

Conclusions—Multiple lines of investigation indicate that NAc core astrocytes exist in a hypo-reactive state following cocaine self-administration and extinction. Decreased association

Address correspondence to: Kathryn J. Reissner, PhD, UNC Chapel Hill, CB3270 235 E. Cameron Ave., Chapel Hill, NC 27599. reissner@unc.edu.

*Authors contributed equally

Publisher's Disclaimer: This is a PDF file of an unedited manuscript that has been accepted for publication. As a service to our customers we are providing this early version of the manuscript. The manuscript will undergo copyediting, typesetting, and review of the resulting proof before it is published in its final citable form. Please note that during the production process errors may be discovered which could affect the content, and all legal disclaimers that apply to the journal pertain.

DISCLOSURES

The authors report no biomedical financial interests or potential conflicts of interest.

with synaptic elements may be particularly meaningful, as cessation of chronic cocaine use is associated with changes in synaptic strength and resistance to the induction of synaptic plasticity. We hypothesize that the reduced synaptic colocalization of astrocytes represents an important maladaptive cellular response to cocaine and the mechanisms underlying relapse vulnerability.

Keywords

astrocyte; cocaine; nucleus accumbens; self-administration; colocalization; GFAP

INTRODUCTION

Astrocytes are critically involved in a wide range of physiological processes in the nervous system including synapse formation, synaptic transmission, neuronal energy metabolism, extracellular ion homeostasis, blood flow, and sleep (1–3). In addition, disruption in astrocyte-mediated modulation of neuronal function has been implicated in a wide range of disease processes, including schizophrenia, depression, and addiction (4). Supporting a role for astrocytes in plasticity associated with drug-seeking, Bull and colleagues (5) have shown that activating Gq-coupled signaling via DREADD receptors selectively expressed in NAc core astrocytes inhibits motivation to seek ethanol. Similarly, activating glial Gq-DREADD in the NAc core decreases cued cocaine seeking, an effect mediated by mGluR2/3 receptors (6). In agreement with the proposed role for astrocytes in addiction-related processes, Turner et al (7) reported that transgenic overexpression of a dominant negative component of vesicular release machinery in astrocytes leads to deficits in cocaine reinstatement and conditioned place preference (CPP). Collectively, these and other studies support a role for astrocytes in the cellular mechanisms of addiction (for review see (8)).

A seminal feature of cocaine-induced adaptations in astrocytes is decreased expression and activity of the high affinity glutamate transporter GLT-1 (9). In general, decreased expression of GLT-1 is associated with an increase in reactive astrogliosis following injury, ischemia and neural degeneration (10–12), raising the hypothesis that NAc astrocytes may exist in a state of reactive astrogliosis following self-administration and extinction. Indeed, astrocyte activation has been reported following noncontingent administration of cocaine, methamphetamine, and opiates (13–16) and is associated with methamphetamine-induced neurotoxicity and opiate-induced hypersensitivity to pain (17, 18). Further, astrocyte activation is generally characterized by increased expression of the intermediate filament protein, glial fibrillary acidic protein (GFAP) (19). Thus, we hypothesized that operant cocaine self-administration and extinction would similarly impact GFAP expression as well as structural aspects of astrocyte physiology.

However, results from a series of complementary approaches indicated opposite effects of cocaine self-administration. Cocaine self-administration and extinction training rendered NAc astrocytes in a state characterized by decreased GFAP expression, surface area, volume, and decreased colocalization with synapsin I. The cocaine-mediated decrease in synaptic colocalization was reversed by administration of ceftriaxone, a compound previously shown to restore expression of GLT-1, normalize extrasynaptic glutamate levels, and impair cocaine reinstatement (9, 20). These data expand the spectrum of the adaptations that occur in

response to chronic cocaine exposure in the central nervous system, and infer broad implications toward a more complete understanding of the cocaine-induced adaptations in synaptic communication and plasticity responsible for relapse vulnerability.

METHODS AND MATERIALS

Animals and surgical procedures

Male Sprague-Dawley rats (200–250g) were purchased from both Harlan and Charles River. They were housed individually in a temperature-controlled environment on a 12-hour reverse light cycle. Following approximately one week of environmental acclimation, animals were anesthetized with ketamine (100 mg/kg) and xylazine (7 mg/kg), together with ketorolac analgesic (0.28–0.32 mg/kg). A 13 cm silastic catheter (.02 ID, .047 OD, Bio-sil) was implanted into the right jugular vein, exiting the back attached to a 22G canula (Plastics One, Wallingford, CT). Prophylactic antibiotic (Timentin 10 mg/0.1 ml, i.v.) was administered during surgery and four days postoperatively. Catheters were flushed daily with heparin (0.1 ml, 100U/ml) until the end of self-administration.

For imaging of GFP-labeled astrocytes, Lck-GFP expressed under the control of the GfaABC1D promoter in AAV5 (21) was microinjected immediately following catheterization into the nucleus accumbens (1.0 μ L per side, 7.3×10^{12} particles/mL at 0.1 μ L/min) followed by a >15 min diffusion time, and microinjectors were slowly removed over a period of 1–2 min. Virus was microinjected into the NAc core with 26G injectors at a 6° angle at the following coordinate (mm): +1.5 A/P, +2.6 M/L, –7.2 D/V (22). Lck plasmid provided by Baljit Khakh (UCLA) was packaged into AAV5 by the UNC Viral Vector core.

Behavioral training

All operant training (2h/session) was performed in standard rat modular test chambers (Med Associates) at the same time daily. Prior to onset of cocaine self-administration, animals received a food training session (10–12 hrs) in which an active lever press resulted in the administration of a single 45 mg food pellet (Bio-Serv). Following food training, animals were maintained on ~20g chow per day. Self-administration of cocaine was performed on an FR1 schedule, 0.2 mg per infusion paired with a light and tone (70–72 dB). Each infusion was followed by a 20 sec time-out period. Infusions were capped to 40 for the first two days of self-administration, and unrestricted thereafter. Criteria for self-administration was ten days of at least ten cocaine infusions received, followed by 14–16 sessions of extinction training. Cocaine was provided by the NIDA Drug Supply Program. Ceftriaxone (Hospira Worldwide, Inc., Lake Forest, IL 100 mg/kg, i.p.) or vehicle (sterile saline) was administered 30 min prior to the last ten extinction sessions.

Western blotting and immunohistochemistry

For Western blotting, animals were rapidly decapitated 24 hours after the last extinction training session. Tissue was homogenized in 0.32M sucrose, 10mM HEPES (pH 7.4) and protease/phosphatase inhibitor cocktail (Thermo Scientific). Following centrifugation at 1,000 \times g for 10 min, the supernatant was separated into a crude membrane fraction and a crude cytosolic fraction by centrifugation at 12,000 \times g for 20 min. Protein content in the S2

cytosolic fraction was determined by the BCA method (Thermo Scientific) and 10 µg was separated on Bio-Rad BisTris gels and transferred to PVDF membranes, then probed using anti-GFAP (Abcam, ab7779, 1:1000) and anti-GAPDH (Cell Signaling, 1:2000).

For GFAP immunohistochemistry, animals were deeply anesthetized with pentobarbital 24 hours after the last extinction session and perfused with 150 mL 1× PB followed by 200 mL 4% paraformaldehyde (PFA) in 1× PB. Brains were postfixed overnight in 4% PFA in 1× PB. Brains were then transferred to 30% sucrose in 1× PB containing 0.1% NaN₃ for 1–2 days at 4° C, then transferred to 1× PBS and sliced 45 µm on a cryostat. Serial sections (every 6 sections, approximately 2.6 to 1.0 mm anterior to Bregma) were stained for GFAP and visualized using VIP peroxidase substrate as follows: slices were blocked with 10% normal goat serum (NGS) in PBST for an hour and probed at room temp overnight in anti-GFAP (Abcam ab7779, 1:1000) in PBST containing 3% NGS. Slices were washed three times (10 min each) in PBST containing 3% NGS, and incubated for 1 hr at room temperature in biotinylated goat anti-rabbit (Vector Labs, 1:200) in PBST+3% NGS. Sections were then washed twice in PBST+3% NGS, and once in PBS. Slices were incubated at room temp with ABC (Vector Labs) and washed three times in PBS before developed in VIP for 15 seconds (Vector Labs, SK-4600). Slices were washed again in PBS three times (10 minutes/each) followed by 3×10 min wash in PB. Slices were mounted in PB on clean slides (Superfrost Plus) and dried and dehydrated in ethanol, and coverslips were added using Permount.

Stereological cell counts

Quantitative estimates of the total number of GFAP immunoreactive (GFAP-ir) neurons in the NAc core were achieved using an unbiased, stereological cell counting method (23, 24). Briefly, the optical fractionator system consists of a computer-assisted image analysis system including a Nikon Eclipse E-600 microscope hard-coupled to a Prior H128 computer controlled *x-y-z* motorized stage, an Olympus-750 video camera system, a Micron Pentium III 450 computer, and stereological software (Stereoinvestigator, MicroBrightField Inc.; Colchester, VT). The NAc core was outlined under low magnification (10×) on every 6th section through the rostral-caudal extent of the NAc core, and the outlined region was measured with a systematic random design of dissector counting frames (100 × 100 µm). Actual mounted section thickness was found to be 35–37 µm, and a 2 µm guard zone was set for the top and bottom of each section. A 40× objective lens with a 1.4 numerical aperture was used to count cells within the counting frames. The selection of the first section from the NAc core in the rostral position was random and every 6th section was counted — rendering a systematic random design. The total number of GFAP-ir neurons was calculated. Outline contours drawn for NAc core cell counts included areas containing GFAP-ir cells and excluding the anterior commissure.

Astrocyte imaging and colocalization

For fluorescence imaging and colocalization studies, animals were deeply anesthetized with pentobarbital (100 mg/kg), and perfused with 200 mL PB followed by 200 mL 4% paraformaldehyde in 1× PB. Brains were post-fixed for 4–5 hours then transferred to 1×PBS at 4°C. Coronal slices of accumbens (100 µm) were prepared on a vibratome and washed

three times for 5 min in 1× PBS with 2% Triton-X 100, then blocked with 2% NGS in 1× PBS containing 2% Triton-X 100 for 1 hour. Sections were then incubated in 2% NGS-PBST with a rabbit polyclonal antibody against synapsin-1 (Abcam Ab8, 1:500) overnight at 4° C. Sections were washed three times for 5 min in 1× PBST followed by 8 h at room temp with an Alexa-594 conjugated goat anti-rabbit antibody (1:1000, Life Technologies), then washed three more times prior to slide mounting with ProLong Diamond Antifade (Life Technologies).

Z-stacks were acquired using a Leica laser-scanning confocal microscope (Leica SP6 spinning-disk confocal) equipped with the Argon (Ar 488nm), Krypton (Kr 568 nm), and Helium-Neon (He-Ne 633 nm) laser line. GFP was excited using the 488 nm wavelength with a fluorescein filter set, and Alexa 594 labeled synapsin was acquired using the 568 nm wavelength and rhodamine-like filter set. All images were acquired using a 63× oil immersion objective with a 1× digital zoom factor. Acquisition settings were as follows: 1024×1024 frame size, 12 bit image resolution, frame average of 4, and a 2 μm step size. Z-stacks were typically in the range of 22–35 μm. Care was taken to ensure that selected astrocytes were complete through the x, y, and z planes, and non-overlapping (Figure S2). Acquired Z-stacks were exported to BitPlane Autoquant deconvolution software (10 iterations) (25). Colocalization analysis was performed with Bitplane Imaris 3D image analysis software (Zurich, Switzerland) following deconvolution. Lck-GFP images were taken only if viral transduction occurred inside the nucleus accumbens core (22).

Deconvolved 3D z-stacks were analyzed with Imaris software, using the colocalization module. All images are cropped prior to analysis to reduce file size and to isolate single cells. For background correction, GFP and Alexa 594 signals thresholds were set empirically for each image using the 2D scatter plot of the colocalization module (ImarisColoc). Following manual threshold setting, thresholding, each slice of the 3D z-stack was manually checked to ensure accurate determination of colocalization. Thresholded signal intensity/total signal intensity was calculated for each channel. We also recorded the percentage of the dataset colocalized (normalized % colocalization relative to the total number of voxels). Imaging and analysis are astrocytes were performed in an unbiased manner, blind to the groups.

Statistical analyses

Data were analyzed using two-tailed t-tests when analyzing 2 groups (cocaine vs. saline) or 1-way ANOVA followed by Bonferroni corrected multiple comparisons when analyzing 3 groups (cocaine, saline and cocaine + ceftriaxone).

RESULTS

GFAP expression is reduced in the NAc core following cocaine self-administration and extinction

Western blot analysis revealed a significant reduction in GFAP protein levels in the NAc core following cocaine self-administration and extinction when compared to yoked saline controls (Figure 1B, $t_{(14)}=2.967$, $p=0.01$). In contrast, no difference was observed in the

dorsomedial prefrontal cortex, including prelimbic and anteriorcingulate regions (Figure 1B, $t_{(14)}=0.533$, $p=0.60$). The number of GFAP positive cells was independently assessed using stereology in samples immunohistochemically stained for GFAP following saline or cocaine exposure. In agreement with decreased GFAP protein expression, the number of GFAP-positive gray matter astrocytes in the NAc core was significantly reduced following cocaine self-administration and extinction (Figure 1C, D, $t_{(17)}= 2.554$, $p=0.02$).

Accumbens core astrocytes display reduced surface area, volume, and colocalization with a synaptic marker following cocaine self-administration and extinction

Similar to the astrocyte-enriched proteins GLT-1 and xCT (9), we observed decreased expression of GFAP in the NAc core following cocaine self-administration and extinction. However, GFAP represents a relatively minor fraction of overall astrocyte cell volume, and is not localized in peripheral processes where neuronal and synaptic contact is made (26, 27). In order to test the hypothesis that the downregulated GFAP is associated with quantifiable alterations in the morphology of astroglial cells, we transduced cells in the NAc core with an AAV viral vector encoding a membrane-associated GFP (Lck-GFP) under the control of the GFAP promoter. Inclusion of the 11 amino acid Lck tag in the vector used to label astrocytes dramatically enhances the visualization of fine peripheral astrocytic processes by limiting expression the fluorescent label to the plasma membrane (21, 28). Viral infusion produced fields of transduced cells that displayed astroglial morphology through out the NAc core (Figure 2, S1). Astrocytes with isolated margins were detectable and selected for analysis (Supplemental Fig S2). In addition to labeling fine astroglial processes, GFP-expressing cells showed co-registry with GFAP in immunohistochemistry experiments (Figure S1), indicating glial cell-type specific expression of the Lck-GFP.

Animals were trained to respond on an FR1 schedule of reinforcement for cocaine or saline in self-administration experiments. Following self-administration, responding was extinguished with repeated extinction training sessions where lever pressing did not result in the administration of cocaine or saline (Figure 3A). Twenty-four hours following the last extinction session, brain sections were prepared and imaged. Following image acquisition, deconvolution and rendering of an intensity based space-filling model for each astrocyte with the IMARIS software surface area and volume of 4–12 cells per animal were measured (Figure 3B,C). These analyses revealed a 19% decrease in volume (saline 31,242 \pm 1722 microns³, cocaine 25,313 \pm 1110 microns³; ($t_{(26)} = 2.894$, $p=0.008$) (Figure 1D) and a 21% decrease in surface area (saline 27,008 \pm 1035 microns², cocaine 23,279 \pm 1063 microns²; $t_{(26)}= 2.513$, $p=0.019$) following cocaine experience (Figure 3B).

Colocalization analyses of synaptic and astroglial GFP signals were performed using the IMARIS colocalization software toolkit as described previously (29) and consisted of an intensity-based measurement of the co-registry of Lck-GFP and synapsin voxels in a 3D volume. It is important to note that the colocalization measured here does not indicate that synapsin is expressed or embedded in glial cells. Due to the close relationship between fine astroglial processes with neuronal processes (30) we interpret this measurement is an index of proximity by the astrocyte process and synapse. Our data demonstrate a significant decrease in the coregistry of astroglial Lck-GFP and synapsin signals, observed as a 47%

decrease in the percentage of voxels above threshold that contain both signals (Figure 4A, B, D; ($F_{(2,30)} = 4.678, p < 0.05$)). This value is defined by IMARIS as the percentage of region of interest colocalized (%ROI) (saline 0.10 \pm 0.015 %ROI; cocaine 0.05 \pm 0.007 %ROI) (Figure 4D). These data indicate that NAc core astrocytes make fewer proximal contacts with synapses following cocaine exposure. Importantly, we observed no significant difference in the percentage of voxel intensities above threshold for either GFP (saline 43% \pm 2.3%, cocaine 42.8% \pm 1.7%) or synapsin (saline 35% \pm 3.3%, cocaine 36% \pm 1.7%) signals, indicating that a change in expression is unlikely to account for the observed change in colocalization.

Ceftriaxone treatment reverts colocalization of astroglial GFP and synapsin signals marker to saline levels

In order to determine the impact of ceftriaxone treatment on astrocyte surface area, volume, and colocalization with synapsin, a subset of cocaine animals were treated with ceftriaxone or saline vehicle during the last ten days of extinction training. Ceftriaxone has previously been shown to impair reinstatement to cocaine, and restore numerous features of glutamate homeostasis in the NAc, including GLT-1 {Trantham-Davidson, 2012 #29; Sari, 2009 #27; Knackstedt, 2010 #16}. Treatment with ceftriaxone did not revert cocaine-induced decreases in astrocyte volume (cocaine 25,313 \pm 1110 microns³, cocaine + ceftriaxone 22,027 \pm 1056 microns³; $t_{(18)} = 1.780, p=0.092$) or surface area (cocaine 23,279 \pm 1063 microns², cocaine + ceftriaxone 22,220 \pm 1473 microns²; $t_{(18)} = 0.5599, p=0.5825$) in the NAc of cocaine-administering animals (Figure 3B, C); however co-registry of Lck-GFP and synapsin voxels was reverted to saline levels following chronic ceftriaxone treatment during extinction (saline 0.1% ROI coloc \pm 0.015%, cocaine 0.05% ROI coloc \pm 0.007% and cocaine + cef 0.1 %ROI coloc \pm 0.015%) (Figure 4D). The effect of ceftriaxone on astrocytes from saline-administering rats was not investigated, as previous studies have found ceftriaxone to be without effect on GLT-1 levels or extracellular glutamate levels in the NAc of saline-administering animals {Knackstedt, 2010 #16; Trantham-Davidson, 2012 #29}. There was no significant difference in the percentage of signal above threshold for either GFP (cocaine 42.85 \pm 1.782, saline 43 \pm 2.310, coc. + cef 38.67 \pm 1.498) or synapsin (cocaine 35.77 \pm 1.668, saline 34.86 \pm 3.259, coc. + cef 36.33 \pm 2.361) signals between groups.

DISCUSSION

Findings presented herein indicate a significant reduction in astrocyte volume and surface area as well as a significant decrease in the colocalization of astroglial processes with synapsin I in the NAc core following cocaine self-administration and extinction. Consistent with these findings, we observed downregulation of a primary astrocyte-specific structural filament protein GFAP, which is also in agreement with the altered morphometric properties of fluorescently-labeled astrocytes. Interestingly, the cocaine-dependent decrease in synaptic contacts made by astrocytes was reversed by chronic treatment with ceftriaxone during extinction training. Ceftriaxone has previously been shown to impair cocaine reinstatement by restoring measures of glutamate homeostasis in the NAc, an effect mediated largely by its ability to reverse cocaine-induced down regulation of GLT-1 (9, 20, 31, 32). It is interesting

to note that GLT-1 expression is specifically targeted to areas where astrocyte processes are closest to synapses (33) in order to provide efficient glutamate clearance and minimize spillover of synaptically-released glutamate. Moreover, invasion of astroglial processes toward synapses is correlated with magnitude of GLT-1-mediated currents in astrocytes (34). Therefore, the previously reported capacity of ceftriaxone to restore expression of GLT-1 in cocaine-treated subjects (9, 31), combined with our finding that ceftriaxone restores the synaptic localization of astroglial processes argues that ceftriaxone facilitates glutamate uptake by positioning of astroglial processes containing GLT-1 to glutamate synapses. Taken together, our findings indicate that while withdrawal from noncontingent administration of both psychostimulants and opiates leads to evidence of reactive astrocytes characterized by increased GFAP (13, 16), contingent cocaine self-administration and extinction leads to decreased GFAP expression, astrocyte shrinkage and decreased association with synaptic elements. We hypothesize that differences in the regulation of GFAP expression in contingent versus non-contingent models likely arise due to different pharmacokinetic profiles of repeated single large doses of experimenter-administered drug, versus the rate of administration achieved by the animal's control. However, it has been reported that while morphometric features of astrocytes including overall size and complexity are upregulated in the mouse dentate gyrus 24 hours after one non-contingent administrations of cocaine, they are significantly decreased 24 hours following 7 or 14 days of administration {Fattore, 2002 #67}.

It will be interesting to determine whether the changes observed following self-administration and extinction are also observed immediately following the self-administration stage, or are also observed following forced abstinence in lieu of extinction training. The use of extinction in the reinstatement model of drug abuse allows for investigation of enduring cellular changes that contribute to mechanisms of reinstated drug seeking, and has yielded a large body of literature on the cell biology of drug seeking behavior {Bossert, 2013 #68}. Salience of conditioned cues has been well described in human addicts {Peck, 2014 #69}; however, extinction training has yielded marginal success toward long-lasting relapse prevention, perhaps due in part to the complex nature of conditioned cues in an uncontrolled environment. Hence, more detailed investigation of the behavioral conditions in which cocaine-dependent adaptations to astrocytes are observed will inform the mechanism responsible for the observed changes.

Evidence for hypo-reactive astrocytes in psychiatric disease

In cases of injury or inflammation in the brain, decreased GLT-1 expression is often associated with reactive astrocytes and increased GFAP expression (10–12, 19). However, accumulating evidence indicates that in cases of psychiatric disease, specifically anxiety, stress, or depression, decreased GLT-1 expression coincides with decreased GFAP expression. For example, GFAP mRNA is downregulated in both the cortex and hippocampus following chronic, but not acute corticosterone treatment, while the astrocyte marker ALDH1L1 is unchanged (35). Chronic restraint stress results in decreased GFAP as well as GLT-1 expression in the periaqueductal gray (36), and loss of GFAP immunoreactivity as well as astroglial GLT-1 expression has been observed in the prefrontal cortex (37, 38) and hypothalamus (39) in animal models of depression. Further, reductions

in expression of GFAP have been reported in both preclinical animal models of depression, as well as in human postmortem studies of psychiatric disease, most notably depression but also schizophrenia (for review, see (40–42)). Indeed, considerable evidence from the human literature indicates that glial dysfunction and more specifically decreased astrocyte density and astrocyte-mediated glutamate uptake may reflect a cellular feature of the high degree of comorbidity observed between substance use disorders and depression (43).

Experience-dependent adaptations in synaptic localization of astrocyte processes

A similar astroglial adaptation is observed in the supraoptic nucleus (SON) of the hypothalamus during lactation or dehydration (for review see (48, 49). In this case, reduced synaptic and somatic coverage by astrocytes results in impaired glutamate uptake as well as impaired LTP and LTD (50), which closely parallels the capacity of cocaine treatment to simultaneously impair NAc core glutamate uptake and both LTP and LTD (51, 52). As such, the disruption of astroglial morphology and synaptic contact may directly inhibit the ability to induce plasticity, and represent a novel aspect of the drug-induced alterations in NAc core linked to relapse vulnerability.

Astrocytes closely interdigitate with neuronal processes at the level of individual dendritic spines (44), and there is strong evidence for cocaine-induced enhancement of dendritic spine density and head diameter in the NAc core (45–47). Given the reduction in astrocytic processes adjacent to synapses, we propose that cocaine experience causes NAc core astrocytes to move away from synapses, perhaps in part to make room in the neural parenchyma for new spines and the expansion of existing spine heads. Interestingly, while ceftriaxone normalizes glutamate homeostasis, GLT-1 expression, and synaptic colocalization of astrocyte processes, it is without effect on astrocyte volume or surface area, indicating that these adaptations may be mechanistically distinct. Previous studies indicate that GLT-1 expression and surface diffusion in the membrane is controlled by extracellular glutamate and neuronal activity {Murphy-Royal, 2015 #6} {Yang, 2009 #58}. Thus, a priority of investigation is to functionally link these phenomena in the accumbens core with behavioral output (i.e., drug seeking).

Supplementary Material

Refer to Web version on PubMed Central for supplementary material.

Acknowledgments

This work was supported by NIH grant R00DA031790 (KJR) and T32-DA07244 (KLH) and R015369 and DA003906 (PWK). The authors thank Dr. Baljit Khakh for kind gift of Lck-GFP plasmid.

References

1. Allen NJ, Barres BA. Neuroscience: Glia - more than just brain glue. *Nature*. 2009; 457:675–677. [PubMed: 19194443]
2. Frank MG. Astroglial regulation of sleep homeostasis. *Current opinion in neurobiology*. 2013; 23:812–818. [PubMed: 23518138]
3. Parpura V, Heneka MT, Montana V, Oliek SH, Schousboe A, Haydon PG, et al. Glial cells in (patho)physiology. *Journal of neurochemistry*. 2012; 121:4–27. [PubMed: 22251135]

4. Verkhratsky A, Parpura V. Astroglipathology in neurological, neurodevelopmental and psychiatric disorders. *Neurobiology of disease*. 2015
5. Bull C, Syed WA, Minter SC, Bowers MS. Differential response of glial fibrillary acidic protein-positive astrocytes in the rat prefrontal cortex following ethanol self-administration. *Alcoholism, clinical and experimental research*. 2015; 39:650–658.
6. Scofield MD, Boger HA, Smith RJ, Li H, Haydon PG, Kalivas PW. Gq-DREADD Selectively Initiates Glial Glutamate Release and Inhibits Cue-induced Cocaine Seeking. *Biological psychiatry*. 2015
7. Turner JR, Ecke LE, Briand LA, Haydon PG, Blendy JA. Cocaine-related behaviors in mice with deficient gliotransmission. *Psychopharmacology*. 2013; 226:167–176. [PubMed: 23104263]
8. Scofield MD, Kalivas PW. Astrocytic dysfunction and addiction: consequences of impaired glutamate homeostasis. *The Neuroscientist : a review journal bringing neurobiology, neurology and psychiatry*. 2014; 20:610–622.
9. Knackstedt LA, Melendez RI, Kalivas PW. Ceftriaxone restores glutamate homeostasis and prevents relapse to cocaine seeking. *Biological psychiatry*. 2010; 67:81–84. [PubMed: 19717140]
10. Hamby ME, Sofroniew MV. Reactive astrocytes as therapeutic targets for CNS disorders. *Neurotherapeutics : the journal of the American Society for Experimental NeuroTherapeutics*. 2010; 7:494–506. [PubMed: 20880511]
11. Yi JH, Hazell AS. Excitotoxic mechanisms and the role of astrocytic glutamate transporters in traumatic brain injury. *Neurochemistry international*. 2006; 48:394–403. [PubMed: 16473439]
12. Colangelo AM, Alberghina L, Papa M. Astrogliosis as a therapeutic target for neurodegenerative diseases. *Neuroscience letters*. 2014; 565:59–64. [PubMed: 24457173]
13. Bowers MS, Kalivas PW. Forebrain astroglial plasticity is induced following withdrawal from repeated cocaine administration. *The European journal of neuroscience*. 2003; 17:1273–1278. [PubMed: 12670315]
14. Narita M, Suzuki M, Kuzumaki N, Miyatake M, Suzuki T. Implication of activated astrocytes in the development of drug dependence: differences between methamphetamine and morphine. *Annals of the New York Academy of Sciences*. 2008; 1141:96–104. [PubMed: 18991953]
15. Cooper ZD, Jones JD, Comer SD. Glial modulators: a novel pharmacological approach to altering the behavioral effects of abused substances. *Expert opinion on investigational drugs*. 2012; 21:169–178. [PubMed: 22233449]
16. Clark KH, Wiley CA, Bradberry CW. Psychostimulant abuse and neuroinflammation: emerging evidence of their interconnection. *Neurotoxicity research*. 2013; 23:174–188. [PubMed: 22714667]
17. Watkins LR, Hutchinson MR, Milligan ED, Maier SF. "Listening" and "talking" to neurons: implications of immune activation for pain control and increasing the efficacy of opioids. *Brain research reviews*. 2007; 56:148–169. [PubMed: 17706291]
18. Loftis JM, Janowsky A. Neuroimmune basis of methamphetamine toxicity. *International review of neurobiology*. 2014; 118:165–197. [PubMed: 25175865]
19. Anderson MA, Ao Y, Sofroniew MV. Heterogeneity of reactive astrocytes. *Neuroscience letters*. 2014; 565:23–29. [PubMed: 24361547]
20. Trantham-Davidson H, LaLumiere RT, Reissner KJ, Kalivas PW, Knackstedt LA. Ceftriaxone normalizes nucleus accumbens synaptic transmission, glutamate transport, and export following cocaine self-administration and extinction training. *The Journal of neuroscience : the official journal of the Society for Neuroscience*. 2012; 32:12406–12410. [PubMed: 22956831]
21. Shigetomi E, Bushong EA, Haustein MD, Tong X, Jackson-Weaver O, Kracun S, et al. Imaging calcium microdomains within entire astrocyte territories and endfeet with GCaMPs expressed using adeno-associated viruses. *The Journal of general physiology*. 2013; 141:633–647. [PubMed: 23589582]
22. Paxinos, G.; Watson, C. *The Rat Brain in Stereotaxic Coordinates*. 6th. Burlington: Elsevier Academic Press; 2007.
23. Gundersen HJ, Jensen EB. The efficiency of systematic sampling in stereology and its prediction. *Journal of microscopy*. 1987; 147:229–263. [PubMed: 3430576]

24. Boger HA, Middaugh LD, Huang P, Zaman V, Smith AC, Hoffer BJ, et al. A partial GDNF depletion leads to earlier age-related deterioration of motor function and tyrosine hydroxylase expression in the substantia nigra. *Experimental neurology*. 2006; 202:336–347. [PubMed: 16889771]
25. Landmann L. Deconvolution improves colocalization analysis of multiple fluorochromes in 3D confocal data sets more than filtering techniques. *Journal of microscopy*. 2002; 208:134–147. [PubMed: 12423263]
26. Sofroniew MV, Vinters HV. Astrocytes: biology and pathology. *Acta neuropathologica*. 2010; 119:7–35. [PubMed: 20012068]
27. Oberheim NA, Takano T, Han X, He W, Lin JH, Wang F, et al. Uniquely hominid features of adult human astrocytes. *The Journal of neuroscience : the official journal of the Society for Neuroscience*. 2009; 29:3276–3287. [PubMed: 19279265]
28. Benediktsson AM, Schachtele SJ, Green SH, Dailey ME. Ballistic labeling and dynamic imaging of astrocytes in organotypic hippocampal slice cultures. *Journal of neuroscience methods*. 2005; 141:41–53. [PubMed: 15585287]
29. Kupchik YM, Brown RM, Heinsbroek JA, Lobo MK, Schwartz DJ, Kalivas PW. Coding the direct/indirect pathways by D1 and D2 receptors is not valid for accumbens projections. *Nature neuroscience*. 2015
30. Ventura R, Harris KM. Three-dimensional relationships between hippocampal synapses and astrocytes. *The Journal of neuroscience : the official journal of the Society for Neuroscience*. 1999; 19:6897–6906. [PubMed: 10436047]
31. Sari Y, Smith KD, Ali PK, Rebec GV. Upregulation of GLT1 attenuates cue-induced reinstatement of cocaine-seeking behavior in rats. *The Journal of neuroscience : the official journal of the Society for Neuroscience*. 2009; 29:9239–9243. [PubMed: 19625514]
32. Sondheimer I, Knackstedt LA. Ceftriaxone prevents the induction of cocaine sensitization and produces enduring attenuation of cue- and cocaine-primed reinstatement of cocaine-seeking. *Behavioural brain research*. 2011; 225:252–258. [PubMed: 21824497]
33. Yang Y, Gozen O, Watkins A, Lorenzini I, Lepore A, Gao Y, et al. Presynaptic regulation of astroglial excitatory neurotransmitter transporter GLT1. *Neuron*. 2009; 61:880–894. [PubMed: 19323997]
34. Pannasch U, Freche D, Dallerac G, Ghezali G, Escartin C, Ezan P, et al. Connexin 30 sets synaptic strength by controlling astroglial synapse invasion. *Nature neuroscience*. 2014; 17:549–558. [PubMed: 24584052]
35. Carter BS, Hamilton DE, Thompson RC. Acute and chronic glucocorticoid treatments regulate astrocyte-enriched mRNAs in multiple brain regions in vivo. *Frontiers in neuroscience*. 2013; 7:139. [PubMed: 23966905]
36. Imbe H, Kimura A, Donishi T, Kaneoke Y. Chronic restraint stress decreases glial fibrillary acidic protein and glutamate transporter in the periaqueductal gray matter. *Neuroscience*. 2012; 223:209–218. [PubMed: 22890077]
37. Banasr M, Duman RS. Glial loss in the prefrontal cortex is sufficient to induce depressive-like behaviors. *Biological psychiatry*. 2008; 64:863–870. [PubMed: 18639237]
38. Banasr M, Chowdhury GM, Terwilliger R, Newton SS, Duman RS, Behar KL, et al. Glial pathology in an animal model of depression: reversal of stress-induced cellular, metabolic and behavioral deficits by the glutamate-modulating drug riluzole. *Molecular psychiatry*. 2010; 15:501–511. [PubMed: 18825147]
39. Gunn BG, Cunningham L, Cooper MA, Corteen NL, Seifi M, Swinny JD, et al. Dysfunctional astrocytic and synaptic regulation of hypothalamic glutamatergic transmission in a mouse model of early-life adversity: relevance to neurosteroids and programming of the stress response. *The Journal of neuroscience : the official journal of the Society for Neuroscience*. 2013; 33:19534–19554. [PubMed: 24336719]
40. Banasr M, Dwyer JM, Duman RS. Cell atrophy and loss in depression: reversal by antidepressant treatment. *Current opinion in cell biology*. 2011; 23:730–737. [PubMed: 21996102]
41. Cotter DR, Pariante CM, Everall IP. Glial cell abnormalities in major psychiatric disorders: the evidence and implications. *Brain research bulletin*. 2001; 55:585–595. [PubMed: 11576755]

42. Molofsky AV, Krencik R, Ullian EM, Tsai HH, Deneen B, Richardson WD, et al. Astrocytes and disease: a neurodevelopmental perspective. *Genes & development*. 2012; 26:891–907. [PubMed: 22549954]
43. Niciu MJ, Henter ID, Sanacora G, Zarate CA Jr. Glial abnormalities in substance use disorders and depression: does shared glutamatergic dysfunction contribute to comorbidity? *The world journal of biological psychiatry : the official journal of the World Federation of Societies of Biological Psychiatry*. 2014; 15:2–16.
44. Witcher MR, Ellis TL. Astroglial networks and implications for therapeutic neuromodulation of epilepsy. *Frontiers in computational neuroscience*. 2012; 6:61. [PubMed: 22952462]
45. Norrholm SD, Bibb JA, Nestler EJ, Ouimet CC, Taylor JR, Greengard P. Cocaine-induced proliferation of dendritic spines in nucleus accumbens is dependent on the activity of cyclin-dependent kinase-5. *Neuroscience*. 2003; 116:19–22. [PubMed: 12535933]
46. Shen HW, Toda S, Moussawi K, Bouknight A, Zahm DS, Kalivas PW. Altered dendritic spine plasticity in cocaine-withdrawn rats. *The Journal of neuroscience : the official journal of the Society for Neuroscience*. 2009; 29:2876–2884. [PubMed: 19261883]
47. Stefanik MT, Kupchik YM, Kalivas PW. Optogenetic inhibition of cortical afferents in the nucleus accumbens simultaneously prevents cue-induced transient synaptic potentiation and cocaine-seeking behavior. *Brain structure & function*. 2015
48. Piet R, Poulain DA, Oliet SH. Contribution of astrocytes to synaptic transmission in the rat supraoptic nucleus. *Neurochemistry international*. 2004; 45:251–257. [PubMed: 15145540]
49. Theodosis DT, Poulain DA. Activity-dependent neuronal-glia and synaptic plasticity in the adult mammalian hypothalamus. *Neuroscience*. 1993; 57:501–535. [PubMed: 8309521]
50. Panatier A, Theodosis DT, Mothet JP, Touquet B, Pollegioni L, Poulain DA, et al. Glia-derived D-serine controls NMDA receptor activity and synaptic memory. *Cell*. 2006; 125:775–784. [PubMed: 16713567]
51. Moussawi K, Pacchioni A, Moran M, Olive MF, Gass JT, Lavin A, et al. N-Acetylcysteine reverses cocaine-induced metaplasticity. *Nature neuroscience*. 2009; 12:182–189. [PubMed: 19136971]
52. Martin M, Chen BT, Hopf FW, Bowers MS, Bonci A. Cocaine self-administration selectively abolishes LTD in the core of the nucleus accumbens. *Nature neuroscience*. 2006; 9:868–869. [PubMed: 16732275]
53. Vargova L, Sykova E. Astrocytes and extracellular matrix in extrasynaptic volume transmission. *Philosophical transactions of the Royal Society of London Series B, Biological sciences*. 2014; 369:20130608. [PubMed: 25225101]

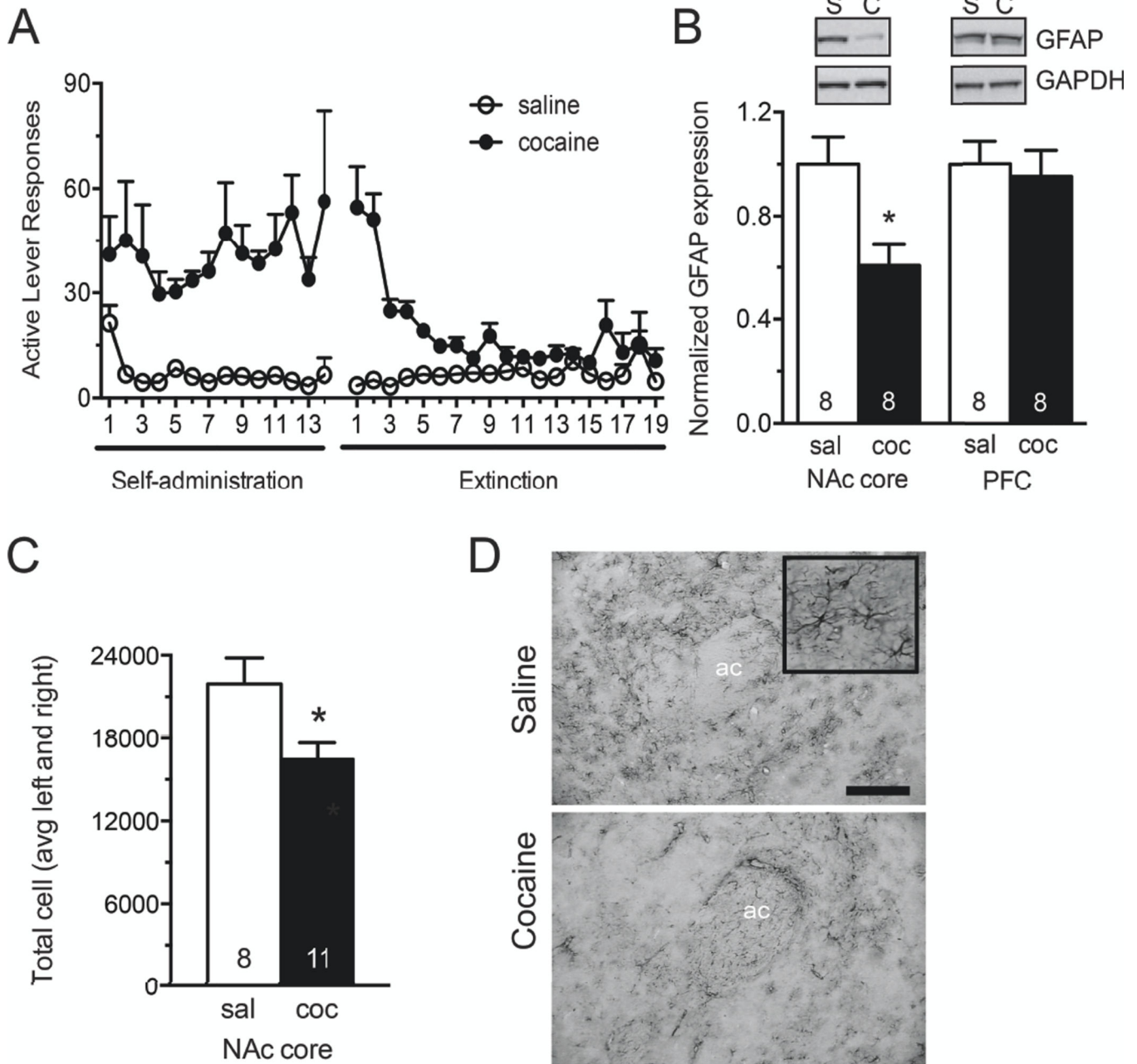


Figure 1. GFAP expression is reduced in NAc core astrocytes following cocaine self-administration and extinction

A) Self-administration and extinction of rats used for Western blotting and GFAP immunohistochemistry. **B)** Western blotting for GFAP in the NAc core S2 subcellular fraction. GFAP signal was normalized to GAPDH loading control, and converted to percent of the saline-administering control group. Western blot analysis revealed a significant decrease in signal following cocaine exposure in the NAc core, while no difference was observed in the PFC. PFC tissue was taken from the dorsomedial prefrontal cortex, including prelimbic and anterior cingulate cortices. **C, D)** Quantitative immunohistochemistry for GFAP was visualized using VIP peroxidase substrate. Unbiased stereological counting was

performed in the NAc core using MicroBrightField StereoInvestigator. Estimated counts are reported as average of left and right hemisphere for each animal. These studies revealed fewer GFAP positive astrocytes in the NAc core following self-administration and extinction. Representative images from saline (top) and cocaine (bottom) administering animals are, shown at 10 \times . 10 \times scale bar, 100 μ m. Inset at 40 \times . *, $p < 0.05$ by Student's unpaired two-tailed t-test. Ac, anterior commissure.

Author Manuscript

Author Manuscript

Author Manuscript

Author Manuscript

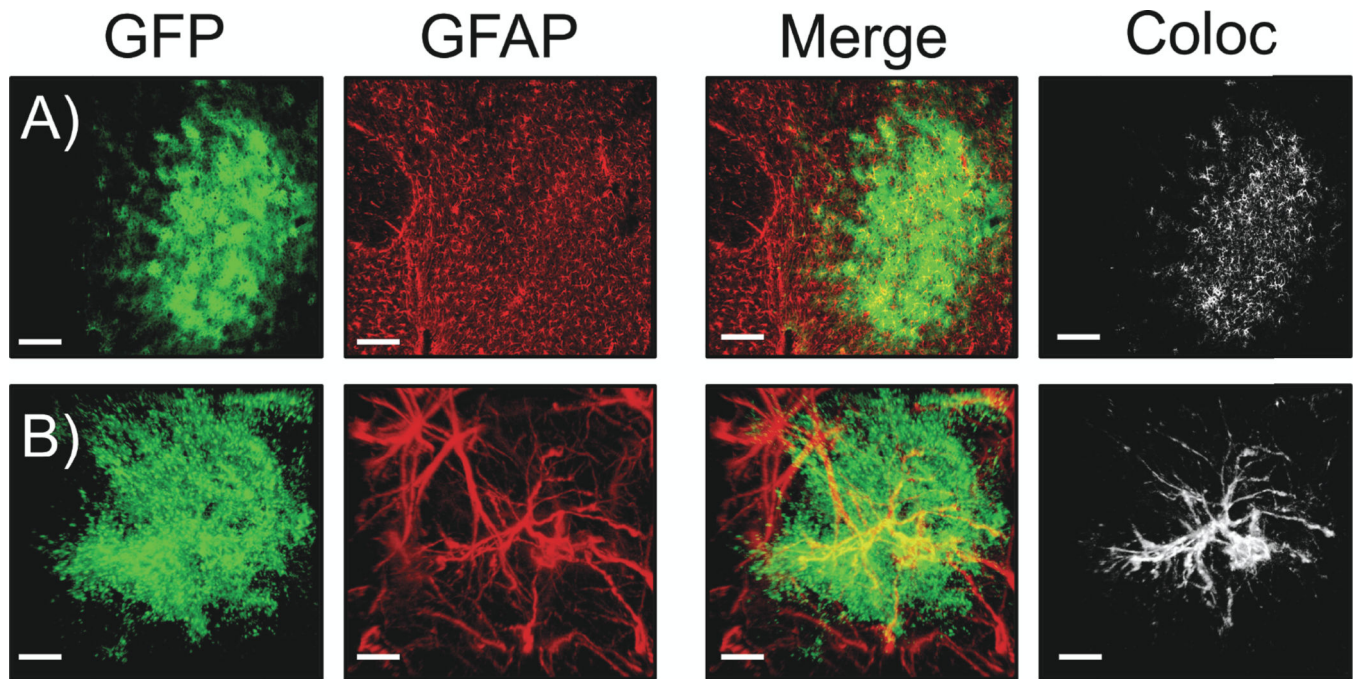


Figure 2. AAV5 GFAP-Lck-GFP drives membrane expression of GFP to NAc core astrocytes
 A) 10 \times images of Lck-GFP transduced NAc core astrocytes. Viral GFP expression is shown in green, GFAP immunohistochemistry is shown in red. The merged image (and the 3D co-localization analysis performed in IMARIS shown in white) demonstrates considerable co-registry of the GFP and GFAP signals, indicating astrocyte specific transduction. The white panel on far right shows voxels containing both viral GFP and GFAP IHC signals. Scale bar is 150 μ m. B) 63 \times Z-series images of a single transduced astrocyte showing membrane-localized GFP expression in green, with GFAP immunohistochemistry in red. Both the merged image and white co-localization analysis show co-localization of the GFP and GFAP signals, again indicating astrocyte specific expression of GFP in the NAc core (see Figure S1 for images from individual planes of the high magnification z-series data set). Scale bar is 10 μ m.

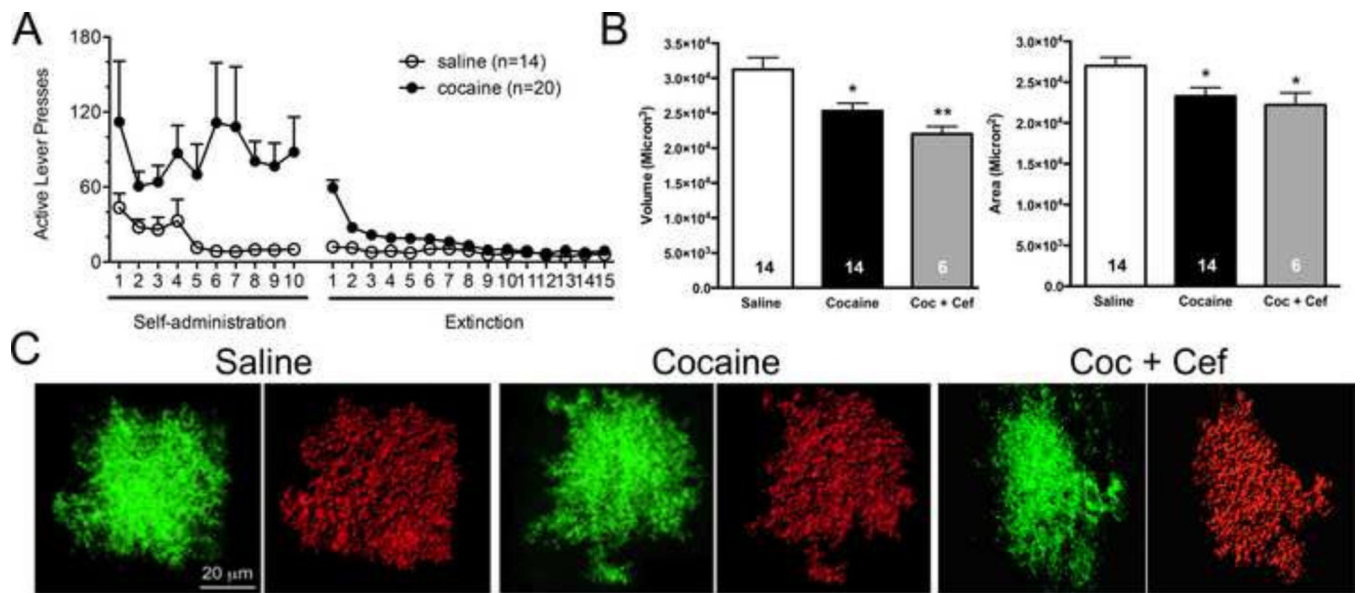


Figure 3. 3D reconstruction of individual NAc core astrocytes following cocaine or saline experience

A) Animals were trained to self-administer cocaine or saline, and were then taken through extinction training. A subset of cocaine-administering rats received either saline or vehicle during extinction training. B) Following rodent behavioral procedures, astrocyte GFP signals from AAV5 GFAP-Lck-GFP transduced cells were used to generate 3D space filling models. Following deconvolution of Z-series datasets, 3D volumes generated by IMARIS were constructed, which recapitulated the shape and contours of astroglial cells transduced with the membrane localized GFP. Space filling models were then used to determine surface area (microns²) and volume (microns³) of NAc core astrocytes following cocaine or saline exposure. C) Cocaine exposure significantly reduced astroglial volume as determined by analysis of IMARIS space filling astrocyte models (shown above in figure 2). Two-tailed t-tests revealed a significant reduction following cocaine exposure. Cocaine exposure also significantly reduced astroglial surface area, * $p < 0.05$, ** $p < 0.01$.

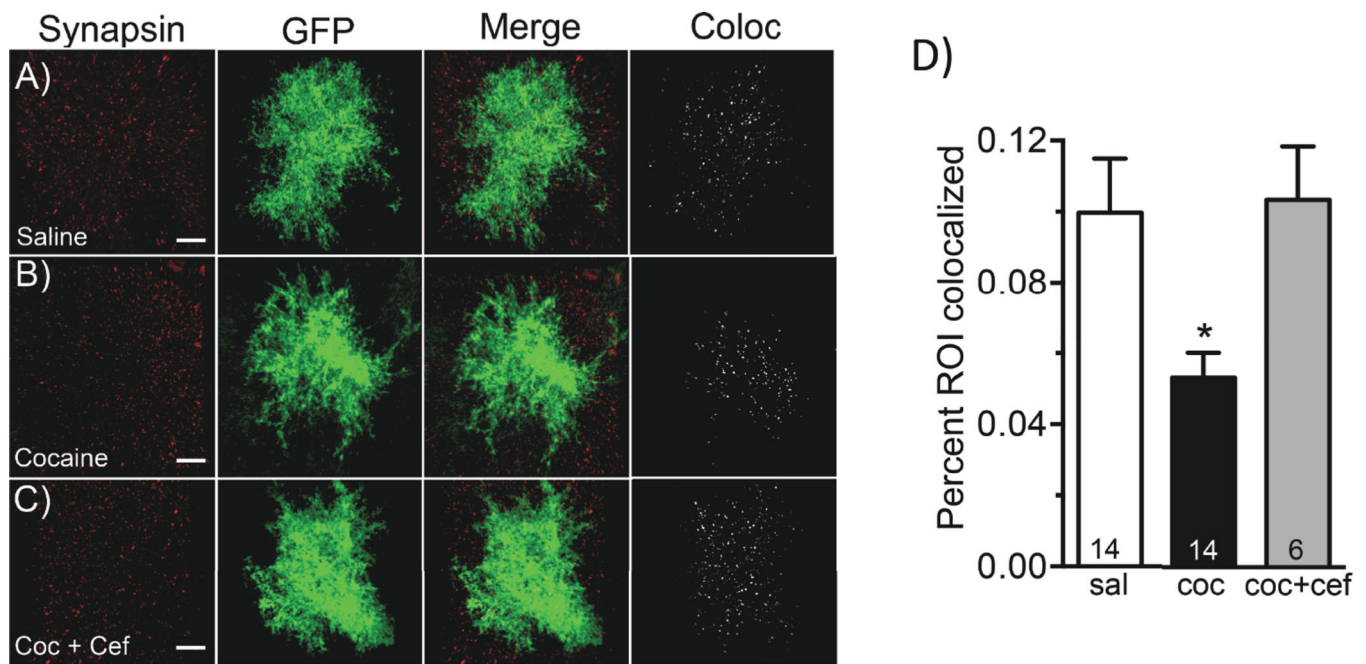


Figure 4. 3D Colocalization analysis of synapsin I with astroglial membrane localized GFP in NAc core astrocytes following cocaine exposure

Brain tissue from animals transduced with the AAV5 GFAP-Lck-GFP virus following saline or cocaine self-administration were stained with the synaptic marker synapsin. Following IHC, individual astrocytes were imaged for both viral GFP expression and synapsin. Using IMARIS, levels of colocalization between synapsin and GFP were assessed using the colocalization toolkit. A) Viral GFP is shown in green for saline-administering animals along with synapsin I in red, a merged image as well as the colocalization channel, where voxels that contain both signals are shown in white. B) This panel shows the same conditions described in A, in animals following cocaine self-administration and extinction training. C) Same conditions described in A, in animals following cocaine self-administration and extinction training with ceftriaxone treatment. D) Using the IMARIS colocalization toolkit, the percentage of the region of interest co-localized was calculated for the astroglial membrane-specific GFP and synapsin signals for 4–12 cells per animal. Cocaine self-administration and extinction training significantly decreased the amount of colocalization of astroglial GFP with synapsin, which is reversed by administration of ceftriaxone during extinction training. * $p < 0.05$.